International Symposium COMODIA 90: 613-618(1990)

Characterization of Soot Clouds and Turbulent Mixing in Diesel Flames by Image Analysis

M.Shioji, K.Yamane, N.Sakakibara and M.Ikegami

Department of Mechanical Engineering
Kyoto University
Yoshida-honmachi
Sakyo-ku, Kyoto 606
Japan

ABSTRACT

Soot clouds formed during combustion in a direct-injection diesel engine were characterized by a laser-light sheet method using an argon-ion laser and high-speed photography. The obtained results suggested that each soot cloud has a very complicated structure that reflects turbulent eddies containing hot but fuel-rich spots. In relation to the soot formation and its reburning, the characteristic scale of turbulence was estimated based on a computer image processing technique, assuming the heterogeneity of the flame luminosity is identical with that of turbulence. Based on this information, the dissipation rate of turbulence and its effect on soot burning are discussed.

INTRODUCTION

Diesel engines for heavy-duty vehicles are demanded to meet new stringent regulations for oxides of nitrogen and particulate emissions. However, there is no knowing how these requirements will be satisfied. To arrive at the solution, we will primarily have to obtain more information on how and why these pollutants are formed during the combustion process.

As has been reported elsewhere (1), the present authors think that the spatial fluctuation, or briefly heterogeneity, of temperature and fuel concentration prevails during the main part of burning and is responsible for the formation of these pollutants. Oxides of nitrogen might be formed in gas pockets having higher temperature than elsewhere, and soot in the interfaces between hot and fuel-overrich parts. Since these parts are subject to turbulent motions and mixing, the temperature and concentrations of each spot would change from time to time.

To look closer at such random behavior and soot formation during the diesel combustion, the present authors undertook high-speed photographic studies on a test engine with optical access, using two different approaches; one being the laser-light sheet method that is capable of detecting soot clouds in the flamelets, and the other being the characterization of turbulent motions of flamelets by an image processing technique. The present paper reports the results of these studies.

As has been widely accepted, high-speed photography is quite helpful in evaluating the combustion process in engines from every aspect in a variety of ways. Among the methods reported are an endoscopic technique (2), stereoscopic photography (3), and a laser-light sheet method (4)(5). In recent years, the laser-light sheet method was developed and successfully applied to visualize the instantaneous flame front on a specified cross-section in a spark-ignition engine. This was achieved by detecting the scattered light intensity from tracer particles that are shaded depending on the gas density. In the present study, the same method was applied to obtain images of soot clouds in diesel flames. Soot clouds were illuminated from a side of the combustion-chamber cavity by a laser light sheet, and the scattered light images were received in the perpendicular direction and recorded in high-speed photographs.

Regarding the characterization of turbulence in flames, the present authors already developed and reported a method of velocimetry using a computer-based picture-processing technique (1)(6). In this method, the average displacement in an observation volume during a time interval between picture frames was given by two-dimensional cross-correlation obtained from two successive shots and the turbulence intensity by the difference between the maxima of the cross- and auto-correlations. In the present study, this method was extended to determine the turbulence scale in the flaming zones to look at the dissipation of turbulent eddies and scaler quantities.

EXPERIMENTAL SET-UP AND PROCEDURE

A Schnürle-scavenged two-cycle single-cylinder engine having a bore of 110mm and a stroke of 120 mm, the same one used in the previous study (1), was rebuilt to allow the laser-light sheet method (LLS). In Fig. 1 the cylinder head and combustion chamber with optical access are shown. Laser light was introduced into the combustion chamber through two quartz windows; one had a ring-shaped spacer inserted between the cylinder head and the liner, and the other a C-shaped window embedded in the piston head so as to form a deep-bowl chamber. A tempered-glass window was installed on the cylinder head to make it possible to observe one of five sprays. In Table 1 the main specifications and operating conditions of the test engine are given.

To obtain a scavenging efficiency as high as in a four-cycle engine, the engine was fired on every other revolution of the engine shaft. The

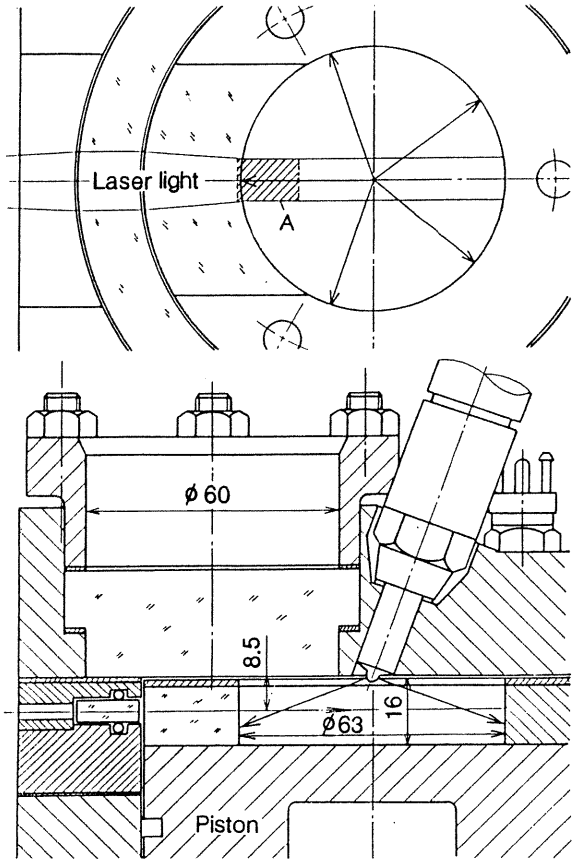

Fig. 1 Cylinder head and piston for photographing combustion

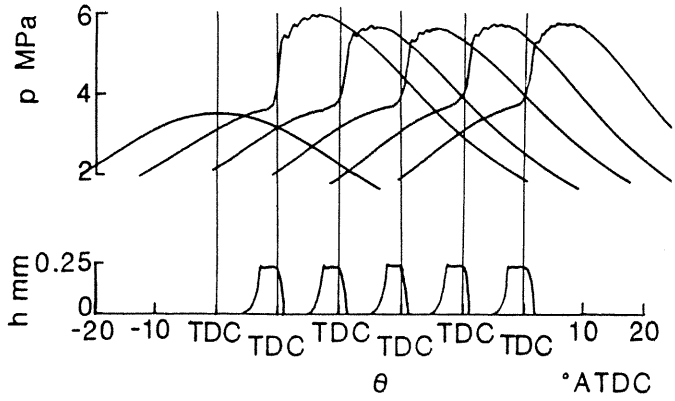

Fig. 2 Consecutive records of cylinder pressure p and injector needle-lift h during photographic run

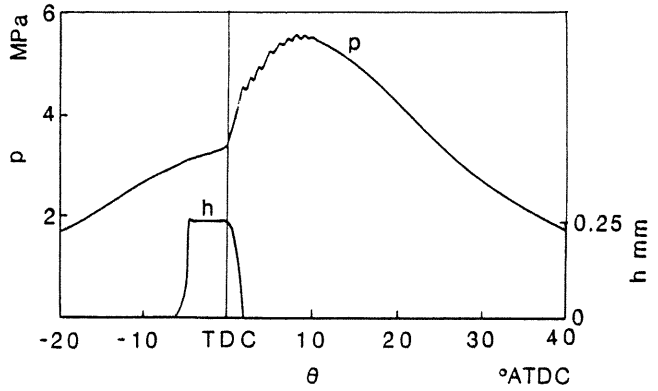

Fig. 3 Cylinder pressure p and injector needle-lift h of the photographed cycle

Table 1 Engine specifications and test conditions

Cylinder bore, stroke	110mm and 120mm
Compression ratio	19.6
Real compression ratio	9.3
Injection pump	Bosch PE2A
Injection nozzle	Five 0.22mm-hole nozzle
Opening pressure	24.5MPa
Spray angle	140 degree
Fuel delivery	35.3mg per fired stroke
Engine speed	760rpm(LLS image) and 860rpm(Direct image)

fuel used was a specially distilled narrow-cut fuel whose main component was n-tridecane; the specific weight was 0.757, the cetane index was 80 and the C/H mass ratio was 5.43. A fuel with such a high cetane index was used to obtain a reasonable length of ignition delay even under somewhat colder conditions during the photographic run, although this measure alone did not give a satisfactory result as will be described later. The scavenge air was supplied by a separate roots blower. A swirl was generated by closing one side of the scavenging ports which directed the scavenging air flow tangentially to the cylinder, and its intensity was regulated by selecting air-delivery ratio. The cylinder pressure and the injector-needle lift during the high-speed photographic run were simultaneously recorded using an AVL-12QP250C type piezoelectric transducer and a Denshi-ohyo Model AEC2225-03S type eddy-current gap sensor, respectively.

A Spectra-Physics Model 2016-05S argon-ion laser having a total light power of 5 W and a wavelength of 514.5 nm was used as the light source for LLS. Using a convex lens of 500 mm focusing length and a cylindrical lens of 25 mm focusing length, the laser beam was focused into a sheet at the position of a distance from the cylinder head of 8.5 mm. The sheet light was introduced to the combustion chamber passing through two quartz windows as shown in Fig. 1. The image of the scattered light was taken in the direction perpendicular to the sheet. The light sheet was about 10 mm in width and 0.230 mm in thickness. A wider illuminating region was preferable, but it was difficult to achieve because the light power became too low to obtain high-speed photographs with a very short exposure time. A Hitachi-koki 16 HD type high-speed camera was used at a set-up speed of 5,000 pictures per second, using Kodak 4-X 7224 16mm monochrome negative films (ASA 400). The LLS photographs were subject to reinforced development at a sensitivity of ASA 6,000 so as to render a very weak scattered-light images. To remove the effect of flame luminosity, an interference filter with a wavelength of 514.5nm and half width of 3nm was inserted on the optical path.

In photographing flames and soot clouds, carbon deposits on the windows seriously deteriorate the quality of the pictures. Therefore, stable combustion should be attained just from the start of the firing run to complete photographing before the carbon deposits grow. This primarily required shortening the length of ignition delay and was met by two measures; one was a motored run over a length of time using a hot scavenge air to warm up every engine part, and the other was the use of a

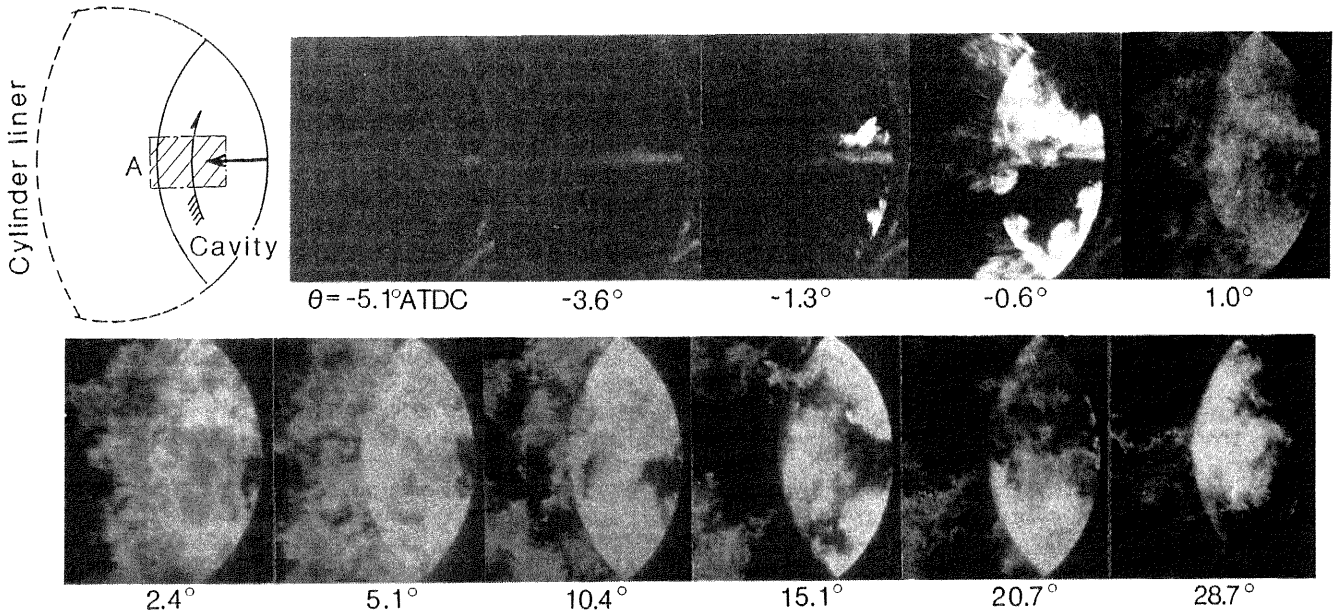

Fig. 4 Direct flame photographs

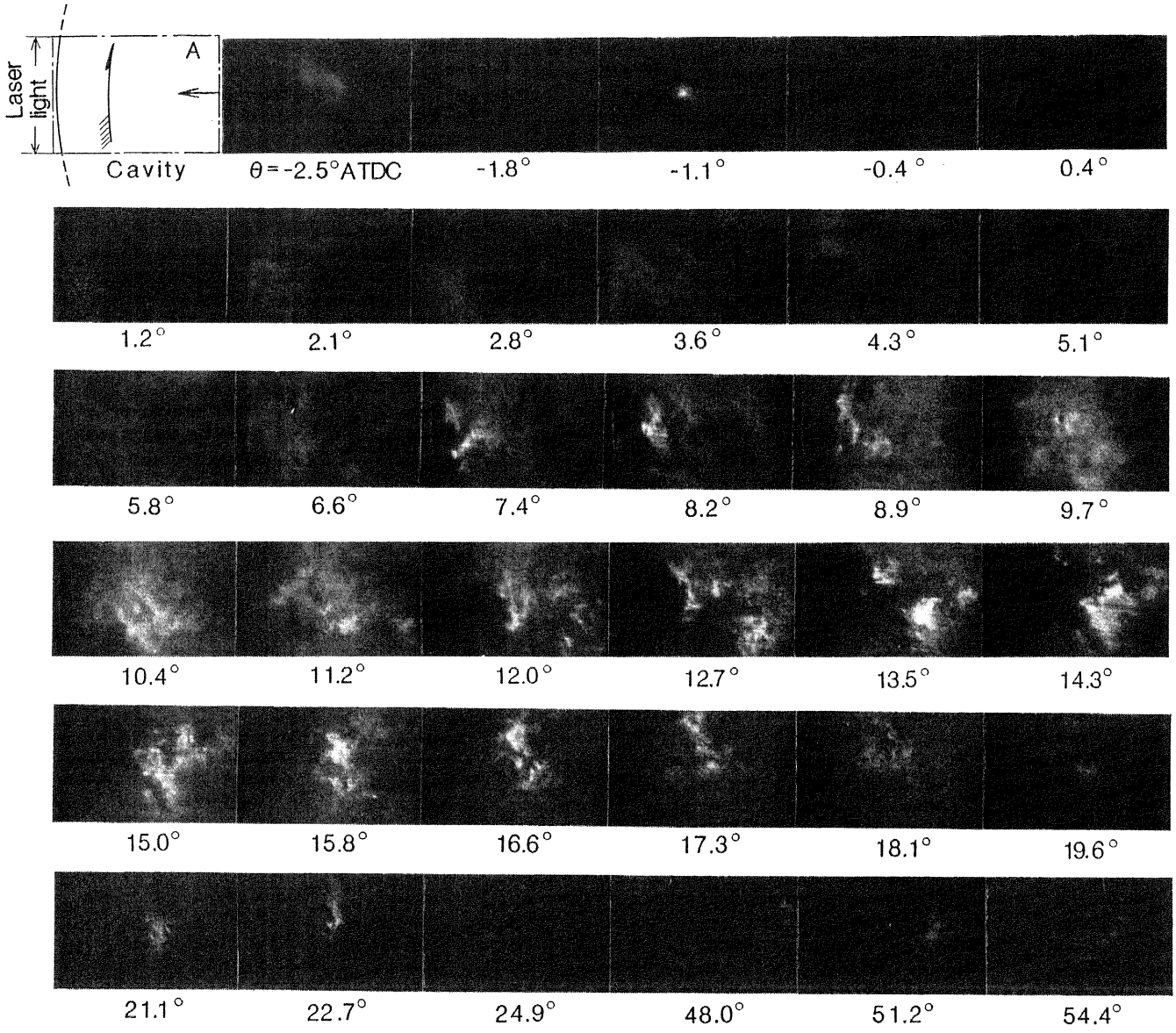

Fig. 5 LLS photographs of soot clouds

mixture of 79% argon and 21% oxygen in place of air only during the fired run. The mixture was fed directly into the suction pipe from a high-pressure gas bottle before the fuel injection was started. Figure 2 shows typical records of cylinder pressure and the injector-needle lift during firing cycles. In the records, no substantial variation is seen in the third and later cycles, indicating that even under such transient running the state of combustion is almost the same as those of the steady run. The high-speed photographs were taken during such a transient state.

LLS VISUALIZATION OF SOOT CLOUDS

Before visualizing the soot particle clouds, the cylinder pressure and the direct photographs of the flame were obtained under a given condition under which the visualization was to be made. In Fig. 3 are shown the cylinder pressure p and injector needle-lift h against crank angle θ for the fourth cycle from the start of firing run. Initial combustion occurs at 5.5°CA after injection starts, and diffusive combustion takes place at 1.5°ATDC when injection terminates. Figure 4 shows the direct flame photographs for the same firing cycle. The spray is visible during crank angles between 6°BTDC and TDC. Ignition first occurs at the position of 20mm distance from the nozzle and in the downstream of the swirl at θ=1.3°BTDC. This crank angle is close to the combustion start from the pressure record. Ignition follows a rapid flame spread and its penetration into the top-clearance area.

Figure 5 shows consecutive photographs of the scattered light, obtained by the laser-light sheet method, for the range of vision of region A in Fig. 1. It should be noted that they were taken under the same condition but not at the same cycle with direct photographs in Fig. 4.

From Fig. 5, the scattered light image due to droplets in the spray is seen between 2°BTDC and TDC, the time of appearance of the image being about 4°CA after the start of injection, at which the spray reaches the laser-illuminated section. Such late appearance of the spray might indicate how fast the gasification of fuel droplets takes place in the spray core. Such a fast gasification of the injected fuel, as already documented in a previous paper (1), may be attributed to the fact that a hot gas produced in the spray mantle is entrained into the spray core, thereby heating the fuel drops.

After the spray image disappears, a region with a lower luminosity gradually expands. Indeed, this background image is due to poor capability of the interference filter in eliminating luminous flames, but this image was fortunately helpful in knowing the extent of flaming zones. It shows that flames are distributed almost in the same region with the luminous flames of direct photographs in Fig. 4. Very bright parts due to soot clouds then become visible at θ=7.4°ATDC. They can clearly be distinguished from the surrounding region of low luminosity. That this image represents soot clouds was evidenced by the fact that if the laser light was off, such luminous parts were no longer observed. Unlike flame observation by direct photographs in Fig. 4, bright portions from soot particles quickly spread just after the onset to cover the entire region of observation.

There is a chance such that until that point very dense soot clouds may exist in front of the view window and hide the illuminated soot zones. The soot clouds might have been observed after the dense clouds in the front disappear. However, this would not be likely because the luminosity of the direct images does not change appreciably before and after the soot clouds appear. For this reason, it would be probable that soot particles first appear on the illuminated section in the observed region about 7°CA after the onset of luminous flames. There are two likely explanations for this fact; one is that until the appearance of soot clouds, the area of observation is near the spray centerline where sooting does not occur because the temperature is not high enough. Visible luminous flames might have been present somewhere outside of this position. The other is that the soot clouds are formed only after a certain length of induction time, even if the temperature of the zone is high enough. Such a phenomenon is well known, for example from shock-tube pyrolysis experiments (7). Unfortunately, it is not certain at the present time which explanation is valid, and further studies would be necessary to answer.

It should be recalled that there is a strong reversed squish motion which makes the gas inside the piston bowl brought into the clearance space on the piston top during the expansion stroke. Since the diameter of the piston cavity is much smaller than the cylinder diameter, the upward gaseous motion at the cross-section under observation has higher relative speed than the downward piston speed. Hence, an observer at the fixed position may watch the fluid moving in the upward direction. Accordingly, a series of soot images would represent traversed instantaneous cross-sectional view of the sooting zones that were formed somewhere in the initial flaming zones around the spray.

The soot-cloud images appearing from θ=6.6°ATDC gradually enlarge, reach the maximum area at 13.5° ATDC, and then decrease in size. Also, it is interesting to note that such clouds are air-borne and seldom formed in the vicinity of the wall of the combustion chamber. Figure 6 presents the contour of the image density I obtained from Fig. 5 by image processing, where I is the degree of opaque-

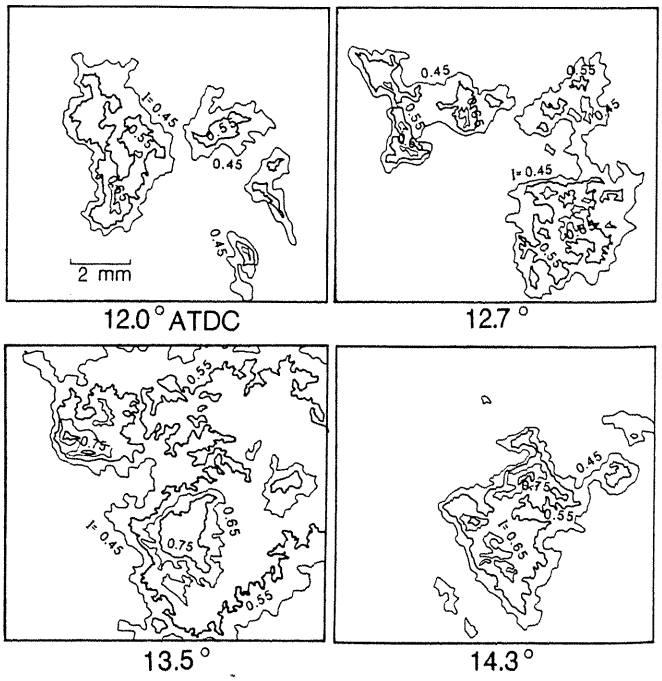

Fig. 6 Optical density distributions of soot clouds

ness of the film negative ranging from 0 to 1; a higher figure indicates a higher scattered-light intensity. It is noted from the figure that the soot cloud has a very complicated and irregular shape, which changes very quickly from picture to picture. Its structure might reflect microscopic turbulent eddies which partition fuel-rich parts. In other words, the profile of the soot clouds would represent the interface between hot, fuel-rich parts and the remainder, segregated in space due to turbulent motion. According to Fig. 6, each soot cloud consists of many clusters each having a size of 2 - 3 mm, which would be in the same order with the scale of the fuel-rich eddies. As has been mentioned earlier, the obtained pictures may give section-to-section view of the soot cloud. For this reason, such soot clouds seem to have a complicated three-dimensional net-like structure.

No scattered light image was detectable from 26°ATDC to 29°ATDC when the metal fixing-plate obstructs the incident laser light. Just after the light path reopens, the soot cloud no longer can be seen. Presumably, burning of soot took place until that time due to turbulent motions. At crank angles later than 48°ATDC, the scattered light images can be observed again. This may be a part of the soot formed in the clearance space that remains and is transferred to the observed section due to certain natural fluid motions. In this case, the soot cloud looks like relatively long strips, having about 2 mm in width, entangled with each other. Its shape changes little from time to time, suggesting that sufficient turbulent motions no longer persist.

TURBULENT MIXING RATE

As has been shown above, the soot formation in the diesel combustion significantly reflects turbulent motion and mixing. Logically speaking, burning of soot particles once formed may proceed, provided that a high rate of turbulent mixing would be preserved until later crank angle degrees, maintaining soot particles to react the oxidizers such as oxygen, carbon monoxide, carbon dioxide and water vapor. This suggests the importance of the dissipation of turbulent eddies with different fuel concentrations during the expansion stroke.

In our previous work (1), the present authors measured the turbulence intensity during the expansion stroke from spatial distributions of the direct high-speed photographs of flames using a computer-based picture-processing technique. Essentially, this method relies on the fact that many flamelets track the fluid motion and hence their temporal change would give information on turbulence. The measured results well elucidated how the turbulence intensity decreases with crank angle and to what extent the swirl intensity and the shape of the combustion chamber affect the turbulence intensity. However, the rate of turbulence dissipation was not obtained during that stage.

The dissipation rate of turbulence, or simply the mixing rate, is proportional to the ratio of rms turbulence intensity u' to a characteristic length scale of turbulence, L. While u' can be given from the direct flame photographs as stated above, L is difficult to determine because either spectrum or auto-correlation of velocity fluctuation is necessary. For this reason, the authors tentatively assumed a similarity between velocity fluctuations and flame-luminosity fluctuations, based on the concept that the microscopic flame pattern would reflect in nature the turbulence field at least in the middle and later burning stages when the combustion chamber becomes almost full of flamelets.

Based on this concept, high-speed photographs were analyzed to obtain u' and L, for three different swirl intensities. The condition of high-speed photographs used for the analysis was the same with those in the previous study (1) but was different from that of the LLS experiment in which an argon-oxygen mixture was used as the cylinder charge.

Figure 7 shows two-dimensional auto-correlation coefficients of light-intensity fluctuation, obtained from the film density, for different swirl ratios r_s. Each contour has a concentric circle around its origin, whose spacings may correspond to the spatial frequency or the scale of the fluctuating image density in each direction. In no swirl case, the spacing between contour lines is wider in the spray direction. In the swirled case more uniform spacings are seen. The contour lines at middle swirl ratio r_s=1.8 are the most dense, indicating that this case will give the smallest scale among three cases.

If the auto-correlation coefficient in a single direction is approximated by an exponential function in terms of distance, the characteristic scale might reasonably be defined as the distance such that the coefficient reaches e^{-1} times the variance of density fluctuation. In the present two-dimensional case, the scale L might be defined as the average of this decay distance for each direction.

Figure 8 shows the mean scale of the optical density fluctuations L, turbulence intensity u', and u'/L, each plotted against crank angle degree, where u'/L is proportional to the mixing frequency under the assumption that L is the same with the turbulence scale. Generally speaking, L slowly increases with crank angle. This tendency would be attributed partly to the natural decay of turbulent eddies, and partly to the decrease in the gas density with the piston motion. It is also interesting to note that L is between 5 mm and 10 mm which is about 2.5 times greater than the scale

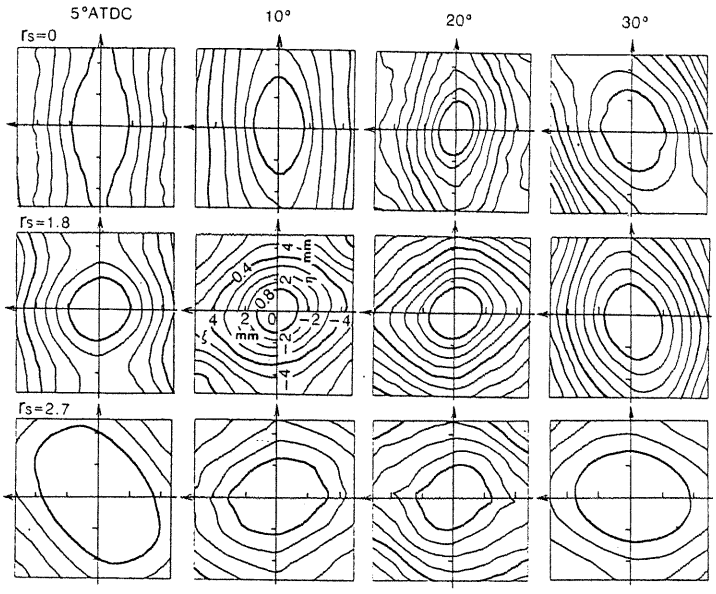

Fig. 7 Two-dimensional auto-correlation coefficients flame-luminosity fluctuations [observation range is a 20 mm square; ζ and η are distances along and across the spray centerline]

of soot clouds obtained in the previous section.

u'/L that is a measure of the mixing frequency decreases with crank angle and becomes very low in the later stages at every r_s.This suggests that mixing of turbulent eddies having different mixture strengths takes place at higher rate in the earlier stages and is slowed down as time goes on. According to the stochastic model for diesel combustion proposed by some of the present authors (8), such a decrease of the mixing rate will lower the rate of heat release since the heterogeneity of concentraton tends to remain. In the same way, soot clouds may survive until later stages, provided the rate of microscopic mixing with the soot oxidizer is not high enough, and hence such soot particles will have a chance to be exhausted without burning.

While u' increases with swirl ratio r_s, u'/L is smaller at r_s=2.7 than at r_s=1.8 because of the significant difference in L. That an intermediate swirl ratio gives the highest mixing rate is quite interesting but beyond explanation at the present time. This might be caused by a certain thermal effect on the turbulent eddies. In fact, the engine performance estimated on the same test engine suggested that the swirl ratio of 2.7 was over-swirled giving a higher concentration of exhaust smoke.

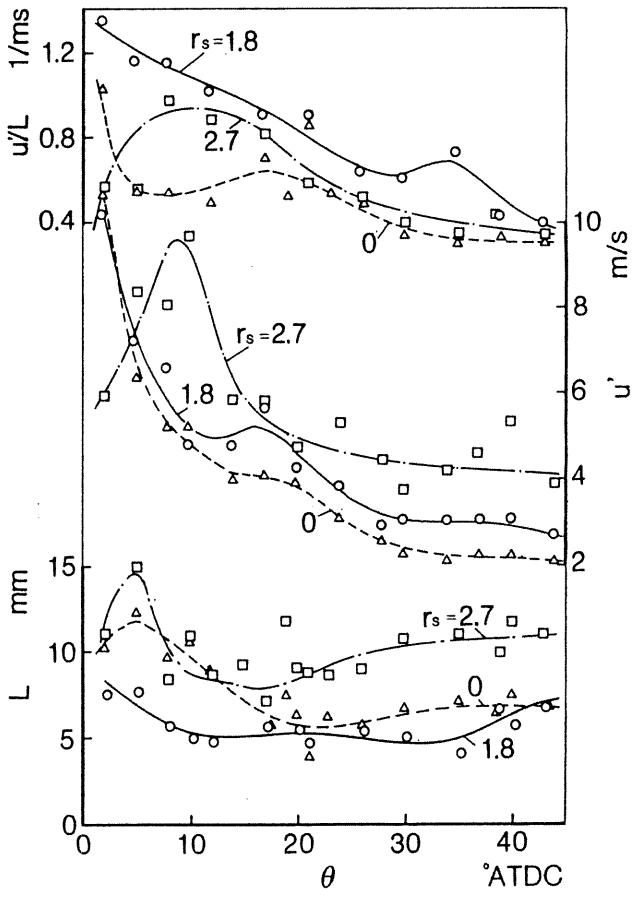

Fig. 8 Scale of density fluctuation L, turbulence intensity u' and the ratio u'/L against crank angle θ for different swirl ratios r_s

CONCLUSIONS

The present study has dealt with heterogeneity and turbulent mixing that would primarily be essential to the diesel combustion process, making use of information obtained from high-speed photographs using the laser-light sheet method for soot-cloud characterization and an image-processing technique for turbulence measurement. These proposed optical methods would be promising for use as diagnosing methods for diesel combustion. What is highlighted in this study would be that soot clouds are formed during combustion and have a complicated three-dimensional structure that reflects turbulent eddies. Also elucidated was the fact that the turbulent mixing rate decreases as crank angle proceeds and hence there is a possibility that soot clouds once formed are frozen if their reburning is hindered at such a low level of mixing rate at the later crank angles.

Acknowledgments: The authors wish to thank Mr. T. Nishii, student of Kyoto University, for his laboratory work. This study was supported by a Grant-in-Aid for Scientific Research (No. 01627006) appropriated in 1989 from the Ministry of Education, Culture and Science of Japan.

REFERENCES

1. M. Ikegami, M. Shioji and T. Kimoto, "Diesel Combustion and the Pollutant Formation as Viewed from Turbulent Mixing Concept," SAE Paper No. 880425, 1988.
2. P. Werlberger and W. P. Cartellieri,"Fuel Injection and Combustion Phenomena in a High Speed DI Diesel Engine Observed by Means of Endoscopic High Speed Photography," SAE Paper No. 870097, 1987.
3. M. Gutmann u. K. Binder, "Neue Aufnahmeverfahren auf dem Gebiet der Hochfrequenz-Filmtechnik," MTZ, Jg. 48, Nr. 1, 1987, S. 21.
4. T. A. Baritaud and R. M. Green, "A 2-D Flame Visualization Technique Applied to the IC Engine," SAE Paper No. 860025, 1986.
5. A. O. zur Loye and F. V. Bracco, "Two-Dimensional Visualization of Premixed-Charge Flame Structure in an IC Engine," SAE Paper No. 870454, SP-715, 1987.
6. M. Shioji, T. Kimoto, M. Okamoto and M. Ikegami, "An Analysis of Diesel Flame by Picture Processing," JSME International Journal, Series II, Vol. 32, No. 3, 1989, p. 434.
7. M. Frenklach, S. Taki, M. B. Durgaprasad, and R. A. Matula, "Soot Formation in Shock-Tube Pyrolysis of Acetylene, Allene, and 1,3-Butadiene," Combust. Flame, Vol. 54, 1983, p. 81.
8. M. Ikegami, M. Shioji, and M. Koike, "A Stochastic Approach to Model the Combustion in Direct-Injection Diesel Engines," Twentieth Symposium (Intern.) on Combustion, The Combustion Institute, 1984, p. 217.